40th Fluid Dynamics Conference and Exhibit
28 June - 1 July 2010, Chicago, Illinois

AIAA 2010-5008

Projection-based model reduction for reacting flows

Marcelo Buffoni* and Karen Willcox†

Massachusetts Institute of Technology, Cambridge, Massachusetts 02139-4307

This paper presents a method based on the proper orthogonal decomposition for model reduction of reacting flow applications. Simulation of reacting flows requires the numerical integration of a system of nonlinear partial differential equations that couples conservation laws, equations of state, and equations describing the chemical source terms. Solution of this coupled system is particularly challenging due to the stiffness of the embedded kinetics and the high computational cost of integrating the nonlinear source term that arises from the chemical models. Existing model reduction approaches are based on separation of reaction timescales, and do not always result in sufficient levels of reduction. The proper orthogonal decomposition approach is combined with the discrete empirical interpolation method to achieve efficient computation of the nonlinear term in the reduced model. Results are shown for parameterized steady and unsteady models describing a two-dimensional premixed H_2-Air flame governed by a nonlinear convection-diffusion-reaction equation.

I. Introduction

Technological improvements in aircraft engines and fuels aimed increased fuel efficiency, reduced pollutant emissions, and reduced greenhouse gas production require a detailed knowledge of the combustion process. In this context, computational methods play a significant role. They reduce design effort, testing time and cost by minimizing the need to build hardware and run laboratory experiments. However, despite a rapid increase in computational power and hardware capacity, numerical simulation of reacting flows with detailed chemistry remains a challenging and computationally demanding task. Simulation of reacting flows requires the numerical integration of a system of nonlinear partial differential equations (PDEs) coupling conservation of mass, momentum and energy; equations of state; and equations describing the chemical source terms. Solving these systems is particularly challenging due to the stiffness of the embedded kinetics and the high computational cost of integrating the nonlinear source term that arises from the chemical models. This paper proposes a model reduction approach that addresses these challenges by providing a systematic means to derive reacting flow models that are fast to solve but retain high-fidelity predictive capability.

Several methods have been developed over the years to reduce the cost of computing the chemical source terms while maintaining accuracy. These methods have originally been developed for spatially homogeneous reactive systems described by large systems of ordinary differential equations (ODEs). Mechanism reduction approaches, based on the separation of fast and slow processes, aim to eliminate the species associated with fast reactions that satisfy quasi-steady state assumptions.[1–4] The ODEs for such species are replaced by algebraic constraints resulting in a reduced model. The computational singular perturbation method (CSP)[3,5] is a general automatic procedure for reduction and analysis of large complex reaction ODE systems. This method relies on the existence of a linearly independent set of basis vectors that decompose the equations governing the chemistry into fast and slow modes. Starting from a trial set of basis vectors, usually the eigenmodes of the Jacobian of the chemical source term, an iterative refinement algorithm is applied to compute an approximation to the ideal basis vectors that decouple the fast and slow subspaces. Once the system is decoupled, the fast modes are approximated by algebraic constraints, leaving only the slow modes in the differential system. Another method that enables automatic separation between slow and fast time scales, based on a dynamical systems approach, is the intrinsic low dimensional manifold (ILDM) approach.[6]

*Postdoctoral Associate, Aerospace Computational Design Laboratory, MIT, mbuffoni@mit.edu. Member AIAA

†Associate Professor of Aeronautics and Astronautics, Aerospace Computational Design Laboratory, MIT, kwillcox@mit.edu. Associate Fellow AIAA

ILDM uses local eigenvector analysis of the Jacobian of the chemical reaction source term to identify the fast time scales and hence the species that can be considered in local equilibrium. The method is usually combined with a tabulation procedure that allows utilization of its results in CFD codes.

Although methods based on time-scale analysis have been applied successfully in combustion simulations[6–9] and atmospheric chemistry,[10–12] their computational cost can be high when many chemical mechanisms are involved. In CSP and ILDM, for instance, slow and fast spaces are identified by analysis of the local Jacobian and its eigenvectors, which need to be updated frequently. Moreover, these methods do not reduce the large dimensionality that arises for models of spatially-varying reactive flows. In such cases, the reaction dynamics are governed by a set of coupled partial differential equations (PDEs). Discretization of the PDEs in space leads to a state space of very high dimension where the states are spatially discrete representations of the reactant concentrations over the computational domain (e.g. values of concentrations at nodal grid points).

Projection-based model reduction is one approach to reduce the complexity of coupled set of PDEs. Reduced-order models based on the proper orthogonal decomposition (POD)[13,14] together with Galerkin projection have been widely used in many applications ranging from fluid mechanics[15–17] to structural mechanics[18,19] to optimal control and optimization.[20–23] This approach employs a Galerkin projection of the large-scale system of equations onto the space spanned by a small set of orthonormal basis functions, the POD modes. In many cases, POD-Galerkin models can achieve significant reductions in model complexity, since the dynamics of interest can often be represented by a small number of POD modes. A significant issue with POD-based reduced models, however, is the generation of a representative data set so that the basis functions are able to capture the short and long term dynamics of the original system. To address this problem, Ref. 24 investigated numerical strategies and performed a sensitivity analysis. More recently, Ref. 25 proposed a combination of POD-Galerkin projection and an adaptation strategy to construct an accurate reduced-order model for a laminar premixed methane-air flame with detailed chemical kinetics.

One challenge with applying the POD-Galerkin method to nonlinear systems is efficient evaluation of the reduced model, since the projected nonlinear term requires computations that scale with the dimension of the original large-scale problem. One approach to address this is the trajectory piecewise-linear scheme, which employs a weighted combination of linear models, obtained by linearizing the nonlinear system at selected points along a state trajectory.[26] Other approaches propose approximating the nonlinear term through selective sampling of a subset of the original equations.[27–30] The missing point estimation approach, based on the theory of gappy POD,[31] is used to approximate nonlinear terms in the reduced model with selective spatial sampling,[28] while the Empirical Interpolation Method (EIM) is used to approximate the nonlinear terms by a linear combination of empirical basis functions for which the coefficients are determined using interpolation.[29,30] Here we use the Discrete Empirical Interpolation Method (DEIM), a discrete version of the EIM that fits well within our POD-Galerkin framework.[32]

In this paper we propose a POD-based approach to obtain efficient reduced-order models of chemically reacting flows. Our method combines the classical Galerkin projection technique with the efficient interpolation procedure of the DEIM. Unlike classical model reduction techniques for reacting flow applications, our approach addresses the reduction of a coupled system of PDEs, achieving substantial reduction in the total number of degrees of freedom. In Section II we present the model reduction framework. In Section III we discuss the governing equations of the model problem to which our approach is applied and the solution methodology, and in Section IV we show results. Finally, Section V concludes the paper.

II. Model reduction technique

Projection-based methods are commonly used to construct reduced-order models (ROMs) of large-scale systems. They derive a ROM by projecting the governing equations onto the subspace spanned by a set of basis vectors.[33] This section describes the projection-based model reduction framework, presents the POD and then describes the empirical interpolation approach used to approximate the nonlinear term.

II.A. Projection framework

Consider the parameterized nonlinear system of ODEs:

$$\dot{\mathbf{x}} = \mathbf{A}\mathbf{x} + \mathbf{F}(\mathbf{x}, \mathbf{p}) \tag{1}$$

with initial conditions

$$\mathbf{x}^0 = \mathbf{x}(0), \tag{2}$$

where $\mathbf{x}(\mathbf{p},t) \in \mathbb{R}^n$ is the state vector of dimension n, $\mathbf{p} \in \mathbb{R}^{n_p}$ is a vector containing n_p input parameters, $\mathbf{x}^0$ is the initial state, $\mathbf{A} \in \mathbb{R}^{n\times n}$ is a constant matrix, $\mathbf{F}(\cdot,\mathbf{p}) : \mathbb{R}^n \to \mathbb{R}^n$ is a nonlinear function of state and parameters, and t denotes time. Systems of ODEs of the form of Eqs.(1-2) arise often from the discretization of PDEs. In such cases n can be very large and the components of the parameter vector $\mathbf{p}$ can describe, for example, coefficients of the PDE and changes in the domain geometry.

To derive the reduced-oder model of Eqs.(1-2), we approximate the original state $\mathbf{x}(\mathbf{p},t)$ as a linear combination of $k \ll n$ basis vectors $\mathbf{v}^i \in \mathbb{R}^n, 1 \le i \le k$,

$$\mathbf{x} \approx \bar{\mathbf{x}} + \mathbf{V}\mathbf{x}_\mathbf{r}, \tag{3}$$

where $\mathbf{V} = [\mathbf{v}_1, \ldots, \mathbf{v}_k] \in \mathbb{R}^{n\times k}$ and $\mathbf{x}_\mathbf{r}(\mathbf{p},t) \in \mathbb{R}^k$ is the vector of the reduced states. Because the basis functions are chosen to satisfy homogeneous boundary conditions, the particular solution $\bar{\mathbf{x}} \in \mathbb{R}^n$ is included when Dirichlet boundary conditions are strongly enforced in the discretized system.

Using Eq.(3) and projecting Eqs.(1-2) onto the subspace spanned by the columns of a left projection matrix $\mathbf{W} \in \mathbb{R}^{n\times k}$ yields the reduced-order model

$$\dot{\mathbf{x}}_\mathbf{r} = \mathbf{A}_{0\mathbf{r}} + \mathbf{A}_\mathbf{r}\mathbf{x}_\mathbf{r} + \mathbf{W}^T\mathbf{F}(\bar{\mathbf{x}} + \mathbf{V}\mathbf{x}_\mathbf{r}, \mathbf{p}) \tag{4}$$

with initial conditions

$$\mathbf{x}_\mathbf{r}^0 = \mathbf{W}^T\mathbf{x}(0), \tag{5}$$

where $\mathbf{W}$ is chosen so that $\mathbf{W}^T\mathbf{V} = \mathbf{I}$ and $\mathbf{I} \in \mathbb{R}^{k\times k}$ is the identity matrix, $\mathbf{A}_{0\mathbf{r}} = \mathbf{W}^T\mathbf{A}\bar{\mathbf{x}} \in \mathbb{R}^k$ and $\mathbf{A}_\mathbf{r} = \mathbf{W}^T\mathbf{A}\mathbf{V} \in \mathbb{R}^{k\times k}$. The k basis vectors can be obtained by many different methods. In this work the basis vectors are constructed using the POD method of snapshots.[14] In this case, the reduced-order model is obtained by Galerkin projection, i.e. $\mathbf{W} = \mathbf{V}$.

II.B. Proper orthogonal decomposition (POD)

The proper orthogonal decomposition (POD), also known as Karhunen-Loève decomposition[34] or principal components analysis,[35] is a procedure that, given a set of solutions (snapshots) at selected times and/or selected parameter values, computes a set of orthonormal basis vectors. Specifically, given a set of l snapshots $\{\hat{\mathbf{x}}_j\}_{j=1}^l$, where $\hat{\mathbf{x}}_j = \mathbf{x}_j - \bar{\mathbf{x}}$, POD computes the set of $k < l$ basis vectors $\{\mathbf{v}_i\}_{i=1}^k$, where $\mathbf{v}_i \in \mathbb{R}^n$ is the ith basis vector. The set of k POD basis vectors solves the minimization problem

$$\min_{\{\mathbf{v}_i\}_{i=1}^k} \sum_{j=1}^{l} \|\hat{\mathbf{x}}_j - \sum_{i=1}^{k} (\hat{\mathbf{x}}_j^T\mathbf{v}_i)\mathbf{v}_i\|_2^2; \quad \text{subject to } \mathbf{v}_i^T\mathbf{v}_j = \delta_{ij} \quad \text{for} \quad 1 \le i,j \le k, \tag{6}$$

where δ_{ij} is the Kronecker delta.

Finding the solution of Eq.(6) is equivalent to finding the left singular vectors of the snapshot matrix $\mathbf{X} = [\hat{\mathbf{x}}_1, \ldots, \hat{\mathbf{x}}_l] \in \mathbb{R}^{n\times l}$. In particular, if the singular value decomposition (SVD) of $\mathbf{X}$ is

$$\mathbf{X} = \mathbf{V}\mathbf{\Sigma}\mathbf{U}^T,$$

where matrices $\mathbf{V} = [\mathbf{v}_1, \ldots, \mathbf{v}_l] \in \mathbb{R}^{n\times l}$ and $\mathbf{U} = [\mathbf{u}_1, \ldots, \mathbf{u}_l] \in \mathbb{R}^{n\times l}$ are orthogonal, $\mathbf{\Sigma} = diag(\sigma_1, \ldots, \sigma_l) \in \mathbb{R}^{l\times l}$ and $\sigma_1 \ge \sigma_2, \ge \cdots \ge \sigma_l > 0$, the POD basis is the set $\{\mathbf{v}_i\}_{i=1}^k$. The POD basis gives the optimal representation, in the least squares sense, of the set of snapshots. The error in representing the snapshots in the basis of dimension k is given by

$$\sum_{j=1}^{l} \|\hat{\mathbf{x}}_j - \sum_{i=1}^{k} (\hat{\mathbf{x}}_j^T\mathbf{v}_i)\mathbf{v}_i\|_2^2 = \sum_{i=k+1}^{l} \sigma_i^2.$$

The quality of the resulting reduced-order model constructed using the POD basis depends a great deal on the choice of the set of snapshots. Treatment of this issue goes beyond the scope of this paper; we refer the interested reader to the works of Veroy *et al.*,[36] Veroy and Patera,[37] Grepl and Patera[38] and Bui-Thanh *et al.*[39]

II.C. Efficient model reduction of nonlinear systems of equations

Although Eq.(4) represents k ODEs with k unknown states, where $k \ll n$, its solution is still expensive. The evaluation of $\mathbf{F}(\mathbf{V}\mathbf{x}_\mathbf{r}(\mathbf{p}))$ and its projection onto the reduced basis depends on the size of the original problem n, as can be seen from the following:

$$\underbrace{\dot{\mathbf{x}}_\mathbf{r}}_{k\times 1} = \underbrace{\mathbf{A}_{0\mathbf{r}}}_{k\times 1} + \underbrace{\mathbf{A}_\mathbf{r}\mathbf{x}_\mathbf{r}}_{k\times 1} + \underbrace{\mathbf{W}^T}_{k\times n}\underbrace{\mathbf{F}(\bar{\mathbf{x}} + \mathbf{V}\mathbf{x}_\mathbf{r}, \mathbf{p})}_{n\times 1}.$$

If large systems are considered, the cost of solving the reduced system of nonlinear equations will be governed by these computations.

The Discrete Empirical Interpolation Method (DEIM),[32] a discrete variant of the Empirical Interpolation Method (EIM) introduced by Barrault *et al.*,[29] provides an effective technique to obtain reduced-order models of nonlinear systems whose online evaluation cost is independent of the size of the original problem. The DEIM consists of an inductive selection procedure that generates an approximation space and a set of interpolation indices that enable the evaluation of the nonlinear function $\mathbf{F}$ at a subset of points $m \ll n$, where n is the dimension of the original ODE system.

The starting point of the procedure is the generation of a set of l snapshots of the nonlinear function, $\{\mathbf{F}_j\}_{j=1}^{l}$, where $\mathbf{F}_j$ is the nonlinear function evaluated at the jth sample conditions of state and parameters. From these l snapshots, a set of POD basis vectors for the nonlinear term is constructed. The nonlinear function $\mathbf{F}$ is then approximated by a linear combination of $m < l$ of these basis vectors,

$$\mathbf{F} \approx \mathbf{\Phi}\boldsymbol{\alpha}, \tag{7}$$

where $\mathbf{\Phi} = [\boldsymbol{\phi}_1, \ldots, \boldsymbol{\phi}_m] \in \mathbb{R}^{n\times m}$ are the POD basis vectors for the nonlinear term, and $\boldsymbol{\alpha} \in \mathbb{R}^m$ are the corresponding expansion coefficients. This approximation cannot be constructed efficiently, since calculation of the expansion coefficients by projection, $\boldsymbol{\alpha} = \mathbf{\Phi}^T\mathbf{F}$, still depends on n. In order to construct a reduced-order representation that is independent of n, we approximate $\boldsymbol{\alpha}$ using a subset $m \ll n$ of the components of $\mathbf{F}$. The subset, $\mathbf{Z} \in \mathbb{R}^m$, of components of $\mathbf{F}$ associated with the basis $\mathbf{\Phi}$ is computed following Ref. 32:

$z_1 = \max\{|\boldsymbol{\phi}_1|\}$
$\mathbf{\Phi} = [\boldsymbol{\phi}_1], \;\; \mathbf{P}[\mathbf{e}_{z_1}], \;\; \mathbf{Z} = [z]$
for $\ell = 2, \ldots, m$
  Solve $(\mathbf{P}^T\mathbf{\Phi})\boldsymbol{\alpha} = \mathbf{P}^T\boldsymbol{\phi}_\ell$ for $\boldsymbol{\alpha}$
  $\mathbf{r} = \boldsymbol{\phi}_\ell - \mathbf{\Phi}\boldsymbol{\alpha}$
  $z_\ell = \max\{|\mathbf{r}|\}$
  $\mathbf{\Phi} \leftarrow [\mathbf{\Phi} \;\; \boldsymbol{\phi}_\ell], \;\; \mathbf{P} \leftarrow [\mathbf{P} \;\; \mathbf{e}_{z_\ell}], \;\; \mathbf{Z} \leftarrow [\mathbf{Z} \;\; z_\ell]^T$
end for

where $\max\{|\cdot|\}$ implies finding the index of the maximum absolute value of $\cdot$, $\{z_1, \ldots, z_m\}$ are the interpolation indices, and $\mathbf{e}_{z_i} = [0, \ldots, 0, 1, 0, \ldots, 0]^T \in \mathbb{R}^n$ is column z_i of the identity matrix $\mathbf{I} \in \mathbb{R}^{n\times n}$ for $i = 1, \ldots, m$.

Once the indices are found, the approximation of $\boldsymbol{\alpha}$ can be computed as

$$\boldsymbol{\alpha} \approx (\mathbf{P}^T\mathbf{\Phi})^{-1}\mathbf{P}^T\mathbf{F}$$

and substituting this approximation in Eq.(7) we obtain

$$\mathbf{F} \approx \mathbf{\Phi}(\mathbf{P}^T\mathbf{\Phi})^{-1}\mathbf{P}^T\mathbf{F}. \tag{8}$$

As a result, the nonlinear term $\mathbf{W}^T\mathbf{F}(\mathbf{V}\mathbf{x}_\mathbf{r}, \mathbf{p})$ in Eq.(4) approximated by DEIM becomes

$$\mathbf{N}_\mathbf{r}(\mathbf{x}_\mathbf{r}, \mathbf{p}) = \mathbf{W}^T\mathbf{\Phi}(\mathbf{P}^T\mathbf{\Phi})^{-1}\mathbf{P}^T\mathbf{F}(\bar{\mathbf{x}} + \mathbf{V}\mathbf{x}_\mathbf{r}, \mathbf{p}), \tag{9}$$

and assuming that $\mathbf{F}$ can be evaluated componentwise at its input vector, Eq. (9) becomes

$$\mathbf{N}_\mathbf{r}(\mathbf{x}_\mathbf{r}, \mathbf{p}) = \underbrace{\mathbf{W}^T\mathbf{\Phi}(\mathbf{P}^T\mathbf{\Phi})^{-1}}_{k\times m}\underbrace{\mathbf{F}(\mathbf{P}^T(\bar{\mathbf{x}} + \mathbf{V}\mathbf{x}_\mathbf{r}), \mathbf{p})}_{m\times 1}. \tag{10}$$

All of the matrices and calculations in Eq.(10) are independent of n, and hence the reduced model is inexpensive to solve. The terms $\mathbf{W}^T\mathbf{\Phi}(\mathbf{P}^T\mathbf{\Phi})^{-1} \in \mathbb{R}^{k\times m}$ and $\mathbf{P}^T(\bar{\mathbf{x}} + \mathbf{V}\mathbf{x}_\mathbf{r}) \in \mathbb{R}^m$ can be precomputed in an offline stage. Therefore the online computation of the reduced-order model requires only the solution of a system of k nonlinear equations with just m evaluations of $\mathbf{F}(\cdot, \mathbf{p})$.

III. Problem formulation and model reduction

We consider a simplified model of a premixed flame at constant and uniform pressure. We also consider a constant and divergence-free velocity field in addition to constant, equal and uniform molecular diffusivities for all species and temperature. Under these assumptions, the system of PDEs governing the evolution of the flame in a domain $\Omega \in \mathbb{R}^2$ with boundaries Γ is given by the following nonlinear convection-diffusion-reaction equation,

$$\frac{\partial \mathbf{x}}{\partial t} = \kappa\Delta\mathbf{x} - U\nabla\mathbf{x} + \mathbf{s}(\mathbf{x}, \mathbf{p}) \quad \text{in } \Omega, \tag{11}$$

with initial and boundary conditions

$$\begin{aligned} \mathbf{x}_D &= \mathbf{x}|_{\Gamma_\mathrm{D}} \\ \mathbf{x}_N &= \mathbf{x}|_{\Gamma_\mathrm{N}} \\ \mathbf{x}(0) &= \mathbf{x}^0, \end{aligned}$$

where $\mathbf{x}(\mathbf{p}, t) = [Y_1, Y_2, \ldots, Y_{n_s}, T]^T \in \mathbb{R}^n$ is the thermo-chemical composition vector, Y_i is the mass fraction of species i, n_s is the total number of species, T is the temperature, κ is the molecular diffusivity, U is the velocity field, $\mathbf{s}(\mathbf{x}, \mathbf{p}) = [s_1, \ldots, s_{ns}, s_T]^T$ is the nonlinear reaction source term and $\mathbf{p}$ is a vector containing input parameters. The total number of degrees of freedom is n, and the subscripts D and N denote Dirichlet and Neumann boundaries respectively. Although quantitative information regarding the flame cannot be extracted from this simplified model problem, it provides a fairly complicated propagation mechanism (convection-diffusion-reaction) that encapsulates the challenges associated with complicated reacting flow problems and thus serves to assess the capabilities of a reduced-order model.

We consider in this work both steady and unsteady problems. The chemistry is modeled by a simple one-step reaction described as

$$\nu_F Y_F + \nu_O Y_O \rightarrow \nu_P Y_P, \tag{12}$$

where Y_F, Y_O and Y_P are the mass fractions of the fuel (F), the oxidizer (O) and the product (P) respectively and ν_F, ν_O and ν_P correspond to their respective stoichiometric coefficients. The nonlinear reaction source term in Eq.(11) is of Arrhenius type and modeled as in Cuenot and Poinsot[40] as:

$$\begin{aligned} s_i(\mathbf{x}, \mathbf{p}) &= -\nu_i \left(\frac{W_i}{\rho}\right) \left(\frac{\rho Y_F}{W_F}\right)^{\nu_F} \left(\frac{\rho Y_O}{W_O}\right)^{\nu_O} A \exp\left(-\frac{E}{RT}\right), \quad i = F, O, P \\ s_T(\mathbf{x}, \mathbf{p}) &= s_P(\mathbf{x}, \mathbf{p}) Q \end{aligned} \tag{13}$$

where A is the pre-exponential factor, W_i is the molecular weight of species i, ρ is the density of the mixture, R is the universal gas constant, T is the temperature, E is the activation energy, Q is the heat of reaction and the parameters $\mathbf{p} = (A, E)$ can vary within the parameter domain $\mathcal{D} \subset \mathbb{R}^2$.

The nonlinear system of PDEs (11) is spatially discretized using the finite difference method (FD). After discretization, for the unsteady case we obtain the following nonlinear system of discrete ordinary differential equations

$$\dot{\mathbf{x}} = \mathbf{K}\mathbf{x} + \mathbf{S}(\mathbf{x}, \mathbf{p}) \tag{14}$$

while for the steady case we obtain the following nonlinear system of discrete algebraic equations

$$\mathbf{K}\mathbf{x} + \mathbf{S}(\mathbf{x}, \mathbf{p}) = 0 \tag{15}$$

where $\mathbf{K} \in \mathbb{R}^{n\times n}$ is a constant matrix corresponding to the FD approximation of the linear spatial differential operators and $\mathbf{S}(\mathbf{x}, \mathbf{p}) \in \mathbb{R}^n$ is the discretized nonlinear source term. The system of nonlinear algebraic equations (15) is solved using Newton's method. For the system of ODEs (14), a second order backward differentiation formula combined with the Newton's method is employed to obtain the solution at each time step.

The model reduction methodology developed in Section II is applied to Eqs.(14) and (15) leading, respectively, to the reduced-order models

$$\dot{\mathbf{x}}_\mathbf{r} = \mathbf{K}_{0\mathbf{r}} + \mathbf{K}_\mathbf{r}\mathbf{x}_\mathbf{r} + \mathbf{R}_\mathbf{r}\mathbf{S}(\mathbf{P}_{0\mathbf{r}} + \mathbf{P}_\mathbf{r}\mathbf{x}_\mathbf{r}, \mathbf{p}) \tag{16}$$

and

$$\mathbf{K}_{0\mathbf{r}} + \mathbf{K}_\mathbf{r}\mathbf{x}_\mathbf{r} + \mathbf{R}_\mathbf{r}\mathbf{S}(\mathbf{P}_{0\mathbf{r}} + \mathbf{P}_\mathbf{r}\mathbf{x}_\mathbf{r}, \mathbf{p}) = 0, \tag{17}$$

where

$$\begin{aligned}
\mathbf{K}_{0\mathbf{r}} &= \mathbf{V}^T\mathbf{K}\bar{\mathbf{x}} && \in \mathbb{R}^k, \\
\mathbf{K}_\mathbf{r} &= \mathbf{V}^T\mathbf{K}\mathbf{V} && \in \mathbb{R}^{k\times k}, \\
\mathbf{P}_{0\mathbf{r}} &= \mathbf{P}^T\bar{\mathbf{x}} && \in \mathbb{R}^m, \\
\mathbf{P}_\mathbf{r} &= \mathbf{P}^T\mathbf{V} && \in \mathbb{R}^{m\times k}, \\
\mathbf{R}_\mathbf{r} &= \mathbf{V}^T\mathbf{\Phi}(\mathbf{P}^T\mathbf{\Phi})^{-1} && \in \mathbb{R}^{k\times m}.
\end{aligned}$$

The matrix $\mathbf{V} = [\mathbf{v}_1, \ldots, \mathbf{v}_k] \in \mathbb{R}^{n\times k}$ contains k POD basis vectors constructed from a set of $l > k$ solution snapshots, $\{\hat{\mathbf{x}}_j = \mathbf{x}_j - \bar{\mathbf{x}}\}_{j=1}^l$, vector $\bar{\mathbf{x}}$ is the arithmetic mean of the set of snapshots, matrix $\mathbf{\Phi} = [\boldsymbol{\phi}_1, \ldots, \boldsymbol{\phi}_m] \in \mathbb{R}^{n\times m}$ contains m POD basis vectors obtained from a set of $l > m$ snapshots of the nonlinear function, $\{\mathbf{S}_j\}_{j=1}^l$, where $\mathbf{S}_j = \mathbf{S}(\mathbf{x}_j, \mathbf{p})$, and matrix $\mathbf{P} \in \mathbb{R}^{n\times m}$ is obtained by applying the DEIM to $\mathbf{\Phi}$. In the present work the set of l solution snapshots corresponds to solutions at l different parameter values for the steady case. For the unsteady case, the set of l solution snapshots is constructed including q solutions, each corresponding to a different time instant, for h different parameter values.

Matrices $\mathbf{K}_\mathbf{r}$, $\mathbf{P}_\mathbf{r}$ and $\mathbf{R}_\mathbf{r}$ and vectors $\mathbf{K}_{0\mathbf{r}}$ and $\mathbf{P}_{0\mathbf{r}}$ are all parameter (and time) independent. Although their computation depends on n and therefore is expensive, they are precomputed once in an *offline* stage. The solution of the reduced-order model, the *online* stage, is then only dependent on k and m, which are usually small (typically 5-100), making it inexpensive.

IV. Numerical results

In this section we present results obtained after applying our model reduction technique to a two-dimensional premixed H_2-Air flame modeled by the system of PDEs (11). The one-step reaction mechanism is given by

$$2H_2 + O_2 \rightarrow 2H_2O,$$

where H_2 is the fuel, O_2 is the oxidizer, H_2O is the product and the nonlinear reaction source term is of the form of Eqs.(13).

For all numerical simulations, the divergence-free velocity field, U, acts in the positive x direction and is set to 50 cm/sec. The diffusivities, κ, are set to 2.0 cm^2/sec. and the density of the mixture, ρ, is set to 1.39×10^{-3} gr/cm^3. The molecular weights, W_i, where i = H_2, O_2, H_2O, are 2.016, 31.9 and 18 gr/mol respectively, the heat of reaction Q = 9800 K and the universal gas constant R = 8.314472 J/(mol K). The system parameter $\mathbf{p} = (A,\ E)$ can take different values within the parameter domain $\mathcal{D} \equiv [5.5\times10^{11},\ 4.5\times10^3] \times [5.5\times10^{13},\ 1.5\times10^4] \subset \mathbb{R}^2$. The set-up for the simulation is schematically shown in Figure 1. On the inflow boundary Γ_2, $Y_{H_2} = 0.0282$, $Y_{O_2} = 0.2259$, and $Y_{H_2O} = 0$ are imposed. On Γ_1 and Γ_3, homogeneous Dirichlet boundary conditions are enforced for the species mass fractions. A temperature of 950 K on Γ_2 and 300 K on Γ_1 and Γ_3 is prescribed. On Γ_4, Γ_5 and Γ_6, homogeneous Neumann conditions for the temperature and mass fractions are imposed. The number of spatial grid points used in the FD discretization is 73 in the x-axis and 37 in the y-axis. The total number of degrees of freedom, n, is 10804. The time step for the unsteady simulations is set to 0.1 milliseconds. As initial condition, $\mathbf{x}(0)$, the domain is considered empty, at a temperature of 300 K and the velocity field is set to zero.

IV.A. Steady case

A set of $l = 100$ solution snapshots are obtained by solving the nonlinear system of algebraic equations (15) for 100 different parameter samples $\mathbf{p}_j$, where $1 \le j \le 100$ and the j^{th} parameter sample corresponds to the j^{th} node of a 10 x 10 uniform grid in the parameter domain $\mathcal{D}$. Figures 2 and 3 show solution snapshots of temperature and H_2O mass fraction for two different parameter samples $\mathbf{p}$.

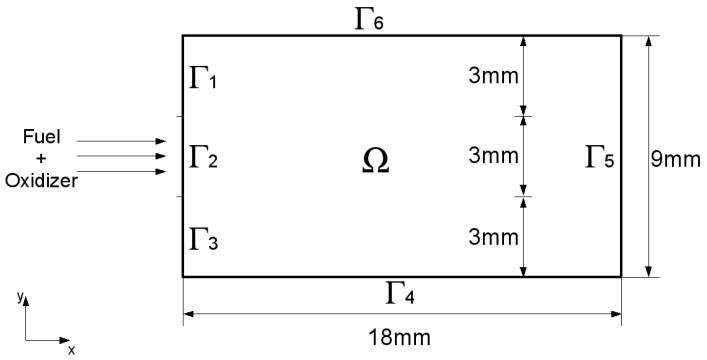

Figure 1. Schematic set-up for the hydrogen-air flame.

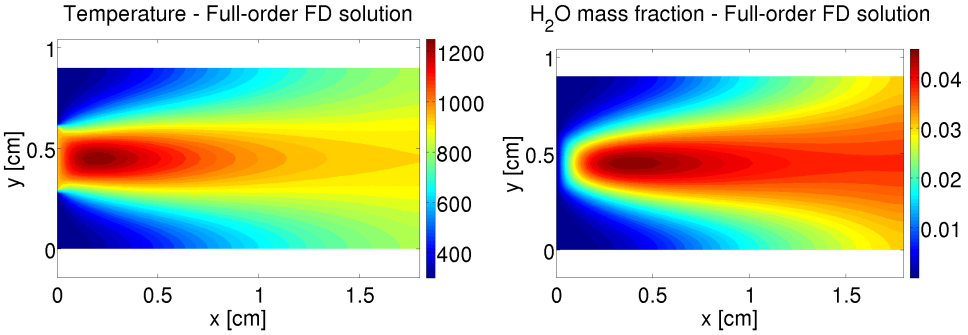

Figure 2. Snapshot for parameter sample $\mathbf{p}_{10} = (\mathrm{A}_{10}, \mathrm{E}_{10}) = (5.5 \times 10^{11}, 4.5 \times 10^{3})$

To test the proposed model reduction technique, the set of 100 snapshots is used to construct POD-DEIM reduced-order models of various sizes, k and m. For each reduced-order model, accuracy is evaluated by measuring the average relative error norm of solutions over a set of test parameters. The test parameters consist of the nodes of a 16 x 16 uniform grid in the parameter domain $\mathcal{D}$ containing different parameter samples from the used to construct the reduced-order models. The same set of test parameters is used to assess performance in terms of online computational time.

Figure 4 presents a comparison of the full and reduced solutions for a parameter sample not used to construct the reduced-order model. The reduced model in this case was constructed using 40 POD basis vectors and 40 interpolation points.

Table 1 and Figure 5 summarize the results obtained with the reduced models. They show the average relative errors in the solutions over the test grid and a comparison of the average online CPU time of the

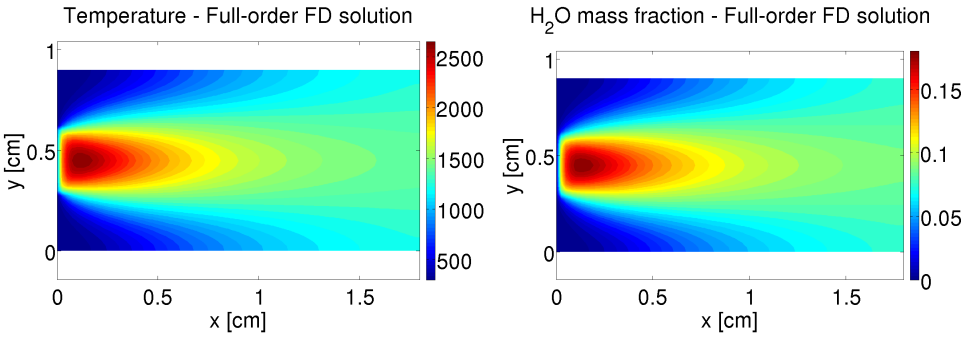

Figure 3. Snapshot for parameter sample $\mathbf{p}_{88} = (\mathrm{A}_{88}, \mathrm{E}_{88}) = (4.895 \times 10^{13}, 6.8333 \times 10^{3})$

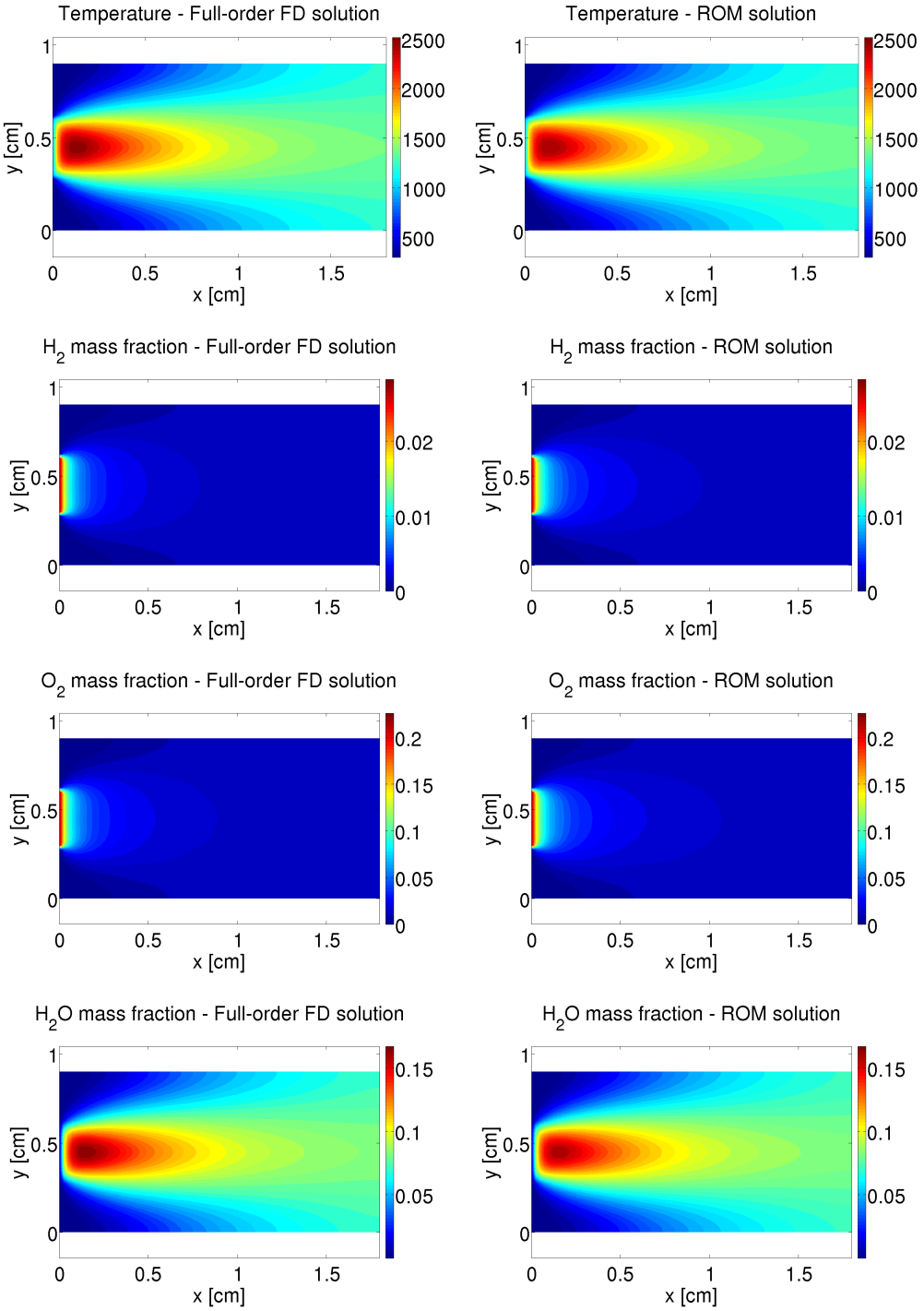

Figure 4. Comparison of full model and reduced model solutions for $\mathbf{p}_{178} = (\mathrm{A}_{178}, \mathrm{E}_{178}) = (4.048 \times 10^{13}, 14.3 \times 10^{3})$). The reduced model was constructed using $k = 40$ and $m = 40$.

POD-DEIM reduced-order models versus the full FD simulation at one of the corners of the test grid. They also show results for a POD reduced-order model. Table 1 shows that for the values of k and m considered, using the POD-DEIM reduced-order model leads to CPU time savings of a factor of approximately 10,000 with respect to the full FD simulation and a factor of approximately 3,000 with respect to the POD model for a similar level of accuracy. Furthermore, even when the reduced-order model is at its higher dimension, the number of degrees of freedom is reduced by a factor of 250. Figure 5 plots the convergence of the

POD			POD-DEIM			
k	Avg. Rel. Error	Online Time	k	m	Avg. Rel. Error	Online Time
1	2.2824e-02	2.9066e-01	1	40	2.2737e-02	1.1823e-04
5	2.3320e-04	2.4486e-01	5	40	2.3561e-04	8.4325e-05
10	1.0315e-05	2.9650e-01	10	40	1.1095e-05	9.0394e-05
15	1.5866e-06	3.5426e-01	15	40	1.6820e-06	1.1038e-04
20	1.9966e-07	2.5036e-01	20	40	5.4281e-07	5.4908e-04
25	1.3298e-07	2.9769e-01	25	40	4.3209e-07	9.2256e-05
30	2.4571e-08	2.2995e-01	30	40	5.0987e-07	9.2579e-05
40	8.5607e-09	2.8202e-01	40	40	4.9660e-07	9.2175e-05

Table 1. Average relative errors (L^2 norm) of solutions computed using the reduced-order models (POD and POD-DEIM) over the parameter test grid and online CPU time for the ROMs as a function of k for $m = 40$. CPU times are normalized with respect to the time required by the full FD model to compute the solution at $\mathbf{p}_{256} = (\mathrm{A}_{256}, \mathrm{E}_{253}) = (5.5 \times 10^{13}, 4.5 \times 10^{3})$.

reduced-order models as the number of POD basis and interpolation points is increased. The figure shows that the number of interpolation points used to approximate the nonlinear term drives the reduced-order model error—increasing the number of state basis functions without a corresponding increase in the number of interpolation points does not result in improved accuracy.

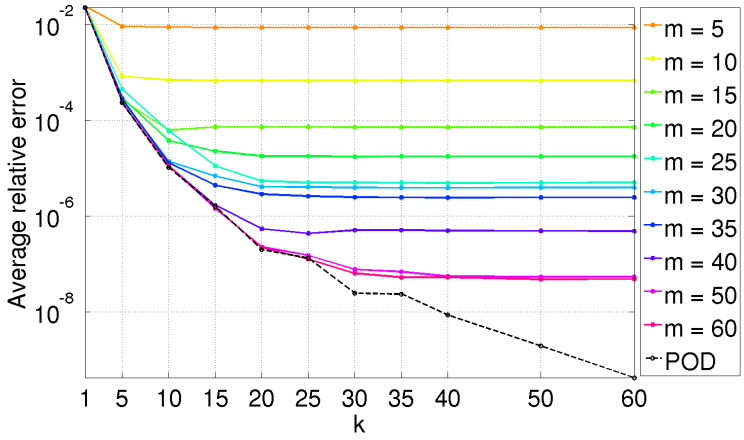

Figure 5. Average relative errors (L^2 norm) of solutions computed using the reduced-order models (POD and POD-DEIM) over the parameter test grid as a function of k and m.

IV.B. Unsteady case

In this case, the set of l solution snapshots is obtained by numerical integration of the nonlinear system of ODEs (14). The snapshots correspond to solutions obtained at each time step. Two different cases are considered here. In the first one, the model reduction technique is used to construct a ROM for a fixed parameter sample $\mathbf{p} = (\mathrm{A}, \mathrm{E})$. In the second case, the technique is employed to construct a ROM that can be used for unsteady simulations and different parameter samples. Starting from the initial condition, $\mathbf{x}^0$, the numerical simulations in the first case are carried out until the system reaches its steady solution while in the second case they are performed for 300 time steps.

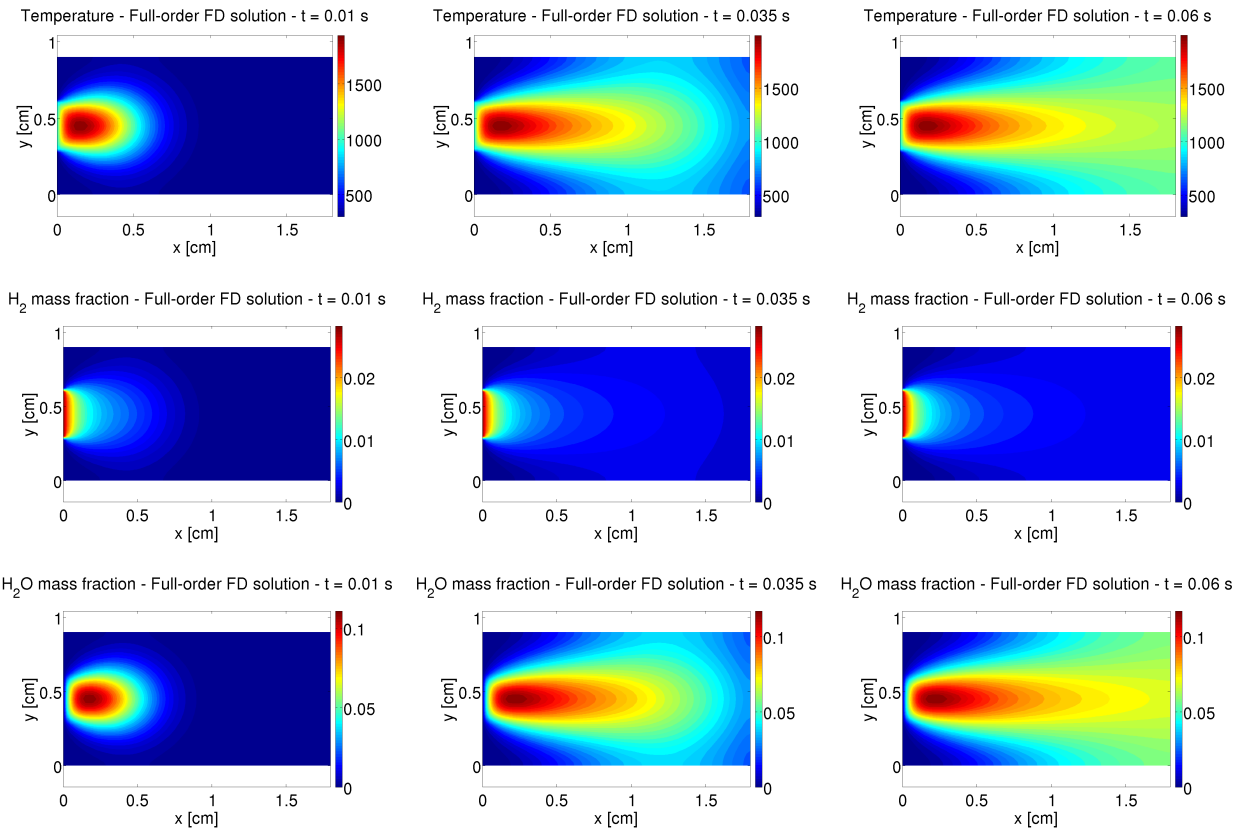

Figure 6. Temperature, H_2 and H_2O mass fraction distribution for three different times during the simulation for $\mathbf{p} = (A, E) = (5.5 \times 10^{12}, 8.0 \times 10^3)$.

IV.B.1. Fixed parameter

A numerical simulation is performed for a fixed parameter sample $\mathbf{p} = (5.5 \times 10^{12}, 8.0 \times 10^3)$. A total of $l = 600$ solution snapshots are obtained, corresponding to 600 time steps. Figure 6 shows temperature and H_2 and H_2O mass fraction distributions on the domain for three different instants of time during the simulation. POD-DEIM reduced-order models of different sizes are constructed using the 600 solution snapshots. A simulation is performed for each ROM and accuracy is assessed by computing the average relative error norm of solutions at each time step. Performance in terms of CPU time required to reach the steady solution is also evaluated.

A summary of the results obtained for the different reduced-order models is shown in Table 2. It can be seen that, as in the steady case, the convergence of the reduced-order models is excellent and errors decrease quickly as the number of POD basis vectors and interpolation points are increased. The results also show that using the POD-DEIM reduced-order models, the CPU time required to reach the steady solution is reduced by an average factor of 1000 with respect to the full-order FD simulation.

Figure 7 shows a comparison of the full and reduced steady solutions and the corresponding absolute error distribution over the computational domain Ω for temperature and H_2O mass fraction.

IV.B.2. Variable parameters

Solution snapshots are obtained from two full-order FD simulations, corresponding to parameter samples $\mathbf{p}_1 = (A_1, E_1) = (2.3375 \times 10^{12}, 5.6255 \times 10^3)$ and $\mathbf{p}_2 = (A_2, E_2) = (6.5 \times 10^{12}, 9.0 \times 10^3)$ respectively. From each simulation, a set of 300 snapshots (one solution at each time step) are computed. The 600 snapshots are then combined in a single set and used to construct the POD-DEIM reduced-order models. The prediction capability of the reduced-order models is assessed by performing simulations for two arbitrarily selected parameter samples included in the parameter domain $\Xi \equiv \mathbf{p}_1 \times \mathbf{p}_2 \subset \mathcal{D} \subset \mathbb{R}^2$ and computing the average relative error norm of the corresponding solutions at each time step. The selected parameter samples for the

POD-DEIM			
k	m	Avg. Rel. Error	Online Time
1	40	2.0227e-01	4.9809e-04
5	40	6.7460e-03	7.9391e-04
10	40	4.4624e-04	8.1592e-04
15	40	1.8409e-05	8.3906e-04
20	40	1.6539e-06	9.6566e-04
25	40	1.5281e-07	8.6716e-04
30	40	7.9887e-08	9.1469e-04
40	40	7.4382e-08	9.6462e-04

Table 2. Average relative errors (L^2 norm) of the solutions and online CPU time for the reduced-order models as a function of k for $m = 40$. CPU times are normalized with respect to the time required by the full FD model to compute the steady solution.

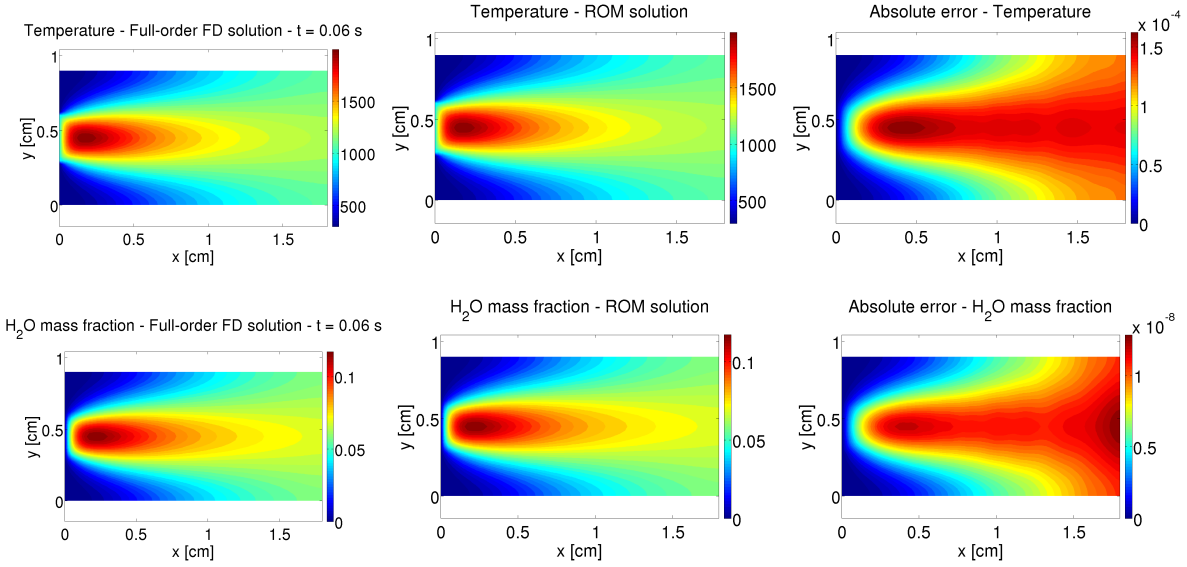

Figure 7. Comparison of full model and reduced model steady solutions for $\mathbf{p} = (\mathrm{A}, \mathrm{E}) = (5.5 \times 10^{12}, 8.0 \times 10^{3})$. The reduced model was constructed using $k = 40$ and $m = 40$.

two test cases are $\mathbf{p}_{t1} = (3.7250 \times 10^{12}, 6.750 \times 10^{3})$ and $\mathbf{p}_{t2} = (5.1125 \times 10^{12}, 7.875 \times 10^{3})$.

Figure 8 shows a comparison of the full and reduced solutions for temperature and mass fraction of H_2O. The solutions are obtained after 300 time steps of the simulation using the parameter sample $\mathbf{p}_{t1}$. The figure also shows the corresponding absolute error distribution over the computational domain Ω for both quantities. In the same manner, Figure 9 presents the results obtained for the parameter sample $\mathbf{p}_{t2}$.

Table 3 shows the results obtained by simulating the reduced-order models for the test parameter samples. It can be seen that the POD-DEIM model is able to accurately predict the simulation for both test parameters, achieving significant reduction in computational time (a factor of approximately 400) and dimensionality (a factor of 125 for the model of higher dimension).

V. Conclusions

This paper presented a model reduction methodology for reacting flow applications based on Galerkin projection, proper orthogonal decomposition and the discrete empirical interpolation method (DEIM). The method provides an offline-online solution strategy that enables a very cheap computation of the derived reduced-order model.

The proposed technique was applied to a one-step simplified two-dimensional combustion problem gov-

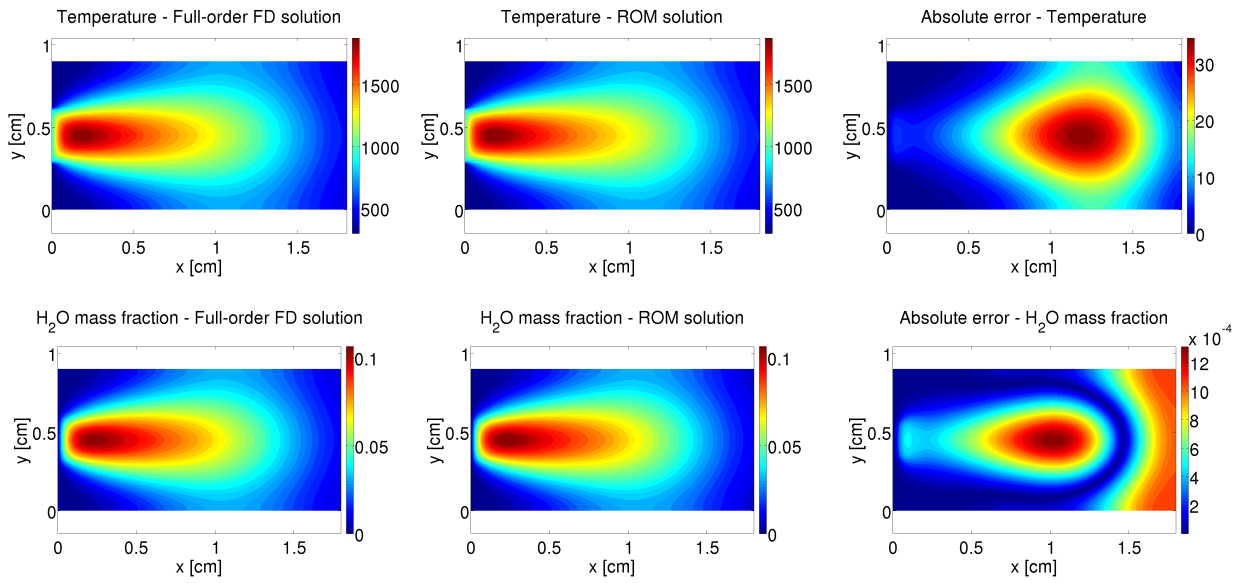

Figure 8. Comparison of full model and reduced model solutions, at time $t = 0.03$, for parameter sample $\mathbf{p}_{t1} = (\mathrm{A}, \mathrm{E}) = (3.7250 \times 10^{12}, 6.750 \times 10^{3})$. The reduced model is constructed using $k = 70$ and $m = 70$.

Test case for $\mathbf{p}_{t1}$				Test case for $\mathbf{p}_{t2}$			
k	m	Avg. Rel. Error	Online Time	k	m	Avg. Rel. Error	Online Time
20	70	1.1304e-02	1.1795e-03	20	60	3.6389e-03	1.2609e-03
30	70	8.9716e-03	1.2550e-03	30	60	5.7951e-03	1.2013e-03
40	70	8.8667e-03	1.3372e-03	40	60	4.9373e-03	1.4860e-03
50	70	8.6059e-03	1.5396e-03	50	60	2.6750e-03	2.3427e-03
60	70	6.1550e-03	2.0105e-03	60	60	1.8835e-03	1.8976e-03
70	70	5.9581e-03	2.2383e-03	70	60	1.4533e-03	2.1587e-03
80	70	5.0581e-03	2.3970e-03	80	60	4.8569e-03	2.6712e-03

Table 3. Average relative errors (L^2 norm) in the predicted solutions for both test parameters and online CPU time for the reduced-order models as a function of k for a fixed value of m. CPU times are normalized with respect to the full FD model simulation.

erned by a nonlinear convection-difussion-reaction PDE. Unlike traditional reduction techniques used for combustion problems, the method addressed reduction of spatially-distributed problems described by PDEs. Numerical results showed that the approach produces accurate models that are substantially smaller than the original systems, achieving orders of magnitude of reduction in computational time.

Acknowledgments

Support for this work has been provided by the Air Force Office of Scientific Research under grant number FA9550-09-1-0239, program manager Dr. Fariba Fahroo, and the Singapore-MIT Alliance Computational Engineering Programme.

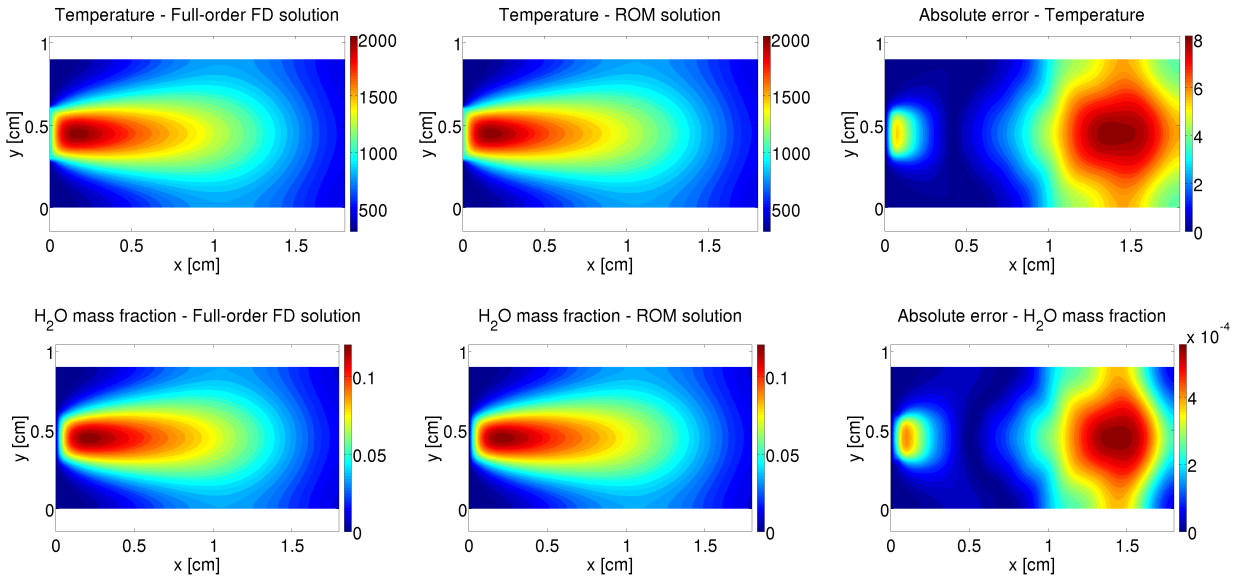

Figure 9. Comparison of full model and reduced model solutions, at time $t = 0.03$, for parameter sample $\mathbf{p}_{t2} = (\mathrm{A}, \mathrm{E}) = (5.1125 \times 10^{12}, 7.875 \times 10^{3})$. The reduced model is constructed using $k = 60$ and $m = 60$.

References

[1]Okino, M. and Mavrovouniotis, M., "Simplification of mathematical models of chemical kinetics," *Chemical Reviews*, Vol. 98, 1998, pp. 391–408.

[2]Hesstvedt, E., Hov, O., and Isaksen, I., "Quasi-steady-state approximations in air pollution modeling: Comparison of two numerical schemes for oxidant prediction," *Int. J. Chem. Kinetics*, Vol. 10, 1978, pp. 971–994.

[3]Lam, S., "Using CSP to understand complex chemical-kinetics," *Combustion Science and Technology*, Vol. 89, 1993, pp. 375–404.

[4]Williams, F., *Combustion Theory*, Addison-Wesley, 1985, New York, 2nd edition.

[5]Goussis, D. and Lam, S., "A study of homogeneous methanol oxidation kinetic using CSP," In *Proc. Comb. Inst.*, Vol. 24, 1992, pp. 113–120.

[6]Maas, U. and Pope, S., "Simplifying chemical kinetics: Intrinsic low dimensional manifolds in composition space," *Combustion and Flame*, Vol. 88, 1992, pp. 239–264.

[7]Maas, U. and Pope, S., "Implementation of simplified chemical kinetics based on intrinsic low-dimensional manifolds," *Proceedings of the Combustion Institute*, Vol. 24, 1992, pp. 103–112.

[8]Maas, U. and Pope, S., "Laminar flame calculations using simplified chemical kinetics based on intrinsic low-dimensional manifolds," *Proceedings of the Combustion Institute*, Vol. 25, 1994, pp. 1349–1356.

[9]Bongers, H., Oijen, J. V., and Goey, L. D., "Intrinsic low-dimensional manifold method extended with diffusion," *Proceedings of the Combustion Institute*, Vol. 29, No. 1, 2002, pp. 1371 – 1378.

[10]Djouad, R. and Sportisse, B., "Solving reduced chemical models in air pollution modelling," *Applied Numerical Mathematics*, Vol. 44, 2000, pp. 49–61.

[11]Løvas, T., Mastorakos, E., and Goussis, D., "Reduction of the RACM scheme using Computational Singular Perturbation Analysis," *J. Geophys. Res.*, Vol. 111, 2006, D13302.

[12]Neophytou, M., Goussis, D., van Loon, M., and Mastorakos, E., "Reduced chemical mechanisms for atmospheric pollution with Computational Singular Perturbation analysis," *Atmospheric Environment*, Vol. 38, 2004, pp. 3661–3673.

[13]Holmes, P., Lumley, J., and Berkooz, G., *Turbulence, coherent structures, dynamical systems and symmetry*, Cambridge University Press, 1998.

[14]Sirovich, L., "Turbulence and the dynamics of coherent structures. Part I,II,III." *Q. Appl. Math.*, Vol. 45, No. 3, 1987, pp. 561–590.

[15]Lucia, D., King, P., and Beran, P., "Reduced order modeling of a two-dimensional flow with moving shocks," *Computers and Fluids*, Vol. 32, 2003, pp. 917–938.

[16]Ma, X. and Karniadakis, G. E., "A low-dimensional model for simulating three-dimensional cylinder flow," *Journal of Fluid Mechanics*, Vol. 458, 2002, pp. 181–190.

[17]Buffoni, M., Camarri, S., Iollo, A., and Salvetti, M., "Low-dimensional modelling of a confined three-dimensional wake flow," *Journal of Fluid Mechanics*, Vol. 569, 2006, pp. 141–150.

[18]Amabili, M., Sarkar, A., and Padoussis, M. P., "Chaotic vibrations of circular cylindrical shells: Galerkin versus reduced-order models via the proper orthogonal decomposition method," *Journal of Sound and Vibration*, Vol. 290, No. 3-5, 2006, pp. 736–762.

[19]Kerschen, G., Golinval, J.-C., Vakakis, A. F., and Bergman, L. A., "The method of proper orthogonal decomposition for dynamical characterization and order reduction of mechanical systems: an overview," *Nonlinear Dynamics*, Vol. 41, 2005, pp. 147–169.

[20]Lall, S., Marsden, J., and Glavaski, S., "Empirical model reduction of controlled nonlinear systems," *Proceedings of the IFAC World Congress*, 1999, pp. 473–478.

[21]Graham, W. R., Peraire, J., and Tang, K. Y., "Optimal control of vortex shedding using low-order models. Part I," *International Journal for Numerical Methods in Engineering*, Vol. 44, 1998, pp. 945–972.

[22]Bui-Thanh, T., Damodaran, M., and Willcox, K., "Aerodynamic Data Reconstruction and Inverse Design Using Proper Orthogonal Decomposition," *AIAA Journal*, Vol. 42, No. 5, 2004, pp. 1505–1516.

[23]Bergmann, M., Cordier, L., and J.-P.Brancher, "Optimal rotary control of the cylinder wake using proper orthogonal decomposition reduced-order model," *Physics of Fluids*, Vol. 17, 2005, pp. 097101.

[24]Sportisse, B. and Djouad, R., "Use of proper orthogonal decomposition for the reduction of atmospheric chemical kinetics," *J. Geophys. Res*, Vol. 59, No. 112, 2007, pp. D06303.

[25]Singer, M. and Green, W., "Using adaptive proper orthogonal decomposition to solve the reaction-diffusion equation," *Applied Numerical Mathematics*, Vol. 59, No. 2, 2009, pp. 272–279.

[26]Rewienski, M. and White, J., "A Trajectory Piecewise-Linear Approach to Model Order Reduction and Fast Simulation of Nonlinear Circuits and Micromachined Devices," *IEEE Transaction on Computer-Aided Design of Integrated Circuits and Systems*, Vol. 22, No. 2, 2003, pp. 155–170.

[27]Bos, R., Bombois, X., and van den Hof, P., "Accelerating large-scale nonlinear models for monitoring and control using spatial and temporal correlations," *Proceedings of American Control Conference*, Boston, USA, 2004.

[28]Astrid, P., Weiland, S., Willcox, K., and Backx, T., "Missing Point Estimation in Models Described by Proper Orthogonal Decomposition," *IEEE Transactions on Automatic Control*, , No. 10, 2008, pp. 2237–2251.

[29]Barrault, M., Maday, Y., Nguyen, N., and Patera, A., "An 'Empirical Interpolation' Method: Application to Effient Reduced-Basis Discretization Of Partial Diffrential Equations," *Comptes Rendus Mathématique. Acadéemie des Sciences, Paris*, Vol. 339, No. 9, 2004, pp. 667–672.

[30]Grepl, M., Maday, Y., Nguyen, N., and Patera, A., "Efficient reduced-basis treatment of nonaffine and nonlinear partial differential equations," *Mathematical Modelling and Numerical Analysis (M2AN)*, Vol. 41, No. 3, 2007, pp. 575–605.

[31]Everson, R. and Sirovich, L., "The Karhunen-Loéve Procedure for Gappy Data," *Journal of the Optical Society of America*, Vol. 12, No. 8, 1995, pp. 1657–1664.

[32]Chaturantabut, S. and Sorensen, D., "Discrete Empirical Interpolation for Nonlinear Model Reduction," Technical Report TR09-05, Department of Computational and Applied Mathematics, Rice University, 2009.

[33]Antoulas, A., Sorensen, D., and Gugercin, S., *A survey of model reduction methods for large-scale systems*, Vol. Structured Matrices in Operator Theory, Numerical Analysis, Control, Signal and Image Processing, chap. 280, American Mathematical Society: Providence, RI, 2001, pp. 193–219.

[34]Loève, M., *Probability Theory*, Van Nostrand, New York, 1955.

[35]Hotelling, H., "Analysis of aComplex of Statistical Variables with Principal Components," *Journal of Educational Psychology*, Vol. 24, No. 7, 1933, pp. 417–441 and 498–520.

[36]Veroy, K., Prud'homme, C., Rovas, D., and Patera, A., "A Posteriori Error Bounds for Reduced-Basis Approximation of Parametrized Noncoercive and Nonlinear Elliptic Partial Differential Equations," *Proceedings of the 16th AIAA Computational Fluid Dynamics Conference*, AIAA Paper 2003-3847, Orlando, FL, 2003.

[37]Veroy, K. and Patera, A., "Certified Real-Time Solution of the Parametrized Steady Incompressible Navier-Stokes Equations: Rigorous Reduced-Basis a Posteriori Error Bounds," *International Journal for Numerical Methods in Fluids*, Vol. 47, No. 8-9, 2005, pp. 773–788.

[38]Grepl, M. and Patera, A., "A Posteriori Error Bounds for Reduced-Basis Approximations of Parametrized Parabolic Partial Differential Equations," *ESAIM. Mathematical Modelling and Numerical Analysis*, Vol. 39, No. 1, 2005, pp. 157–181.

[39]Bui-Thanh, T., Willcox, K., and Ghattas, O., "Model Reduction for Large-Scale Systems with High-Dimensional Parametric Input Space," *SIAM J. Sci. Comput*, Vol. 30, No. 6, 2008, pp. 3270–3288.

[40]Cuenot, B. and Poinsot, T., "Asymptotic and numerical study of diffusion flames with variable Lewis number and finite rate chemistry," *Combustion and Flame*, Vol. 104, 1996, pp. 111–137.